

AperTO - Archivio Istituzionale Open Access dell'Università di Torino

Synthesis and preliminary pharmacological characterisation of a new class of nitrogen-containing bisphosphonates (N-BPs)

This is the author's manuscript

Original Citation:

Availability:

This version is available <http://hdl.handle.net/2318/71632> since 2015-12-22T11:38:21Z

Published version:

DOI:10.1016/j.bmc.2010.02.058

Terms of use:

Open Access

Anyone can freely access the full text of works made available as "Open Access". Works made available under a Creative Commons license can be used according to the terms and conditions of said license. Use of all other works requires consent of the right holder (author or publisher) if not exempted from copyright protection by the applicable law.

(Article begins on next page)



UNIVERSITÀ DEGLI STUDI DI TORINO

This Accepted Author Manuscript (AAM) is copyrighted and published by Elsevier. It is posted here by agreement between Elsevier and the University of Turin. Changes resulting from the publishing process - such as editing, corrections, structural formatting, and other quality control mechanisms - may not be reflected in this version of the text. The definitive version of the text was subsequently published in [*Bioorganic & Medicinal Chemistry*, 18, 2010, doi: 10.1016/j.bmc.2010.02.058].

You may download, copy and otherwise use the AAM for non-commercial purposes provided that your license is limited by the following restrictions:

- (1) You may use this AAM for non-commercial purposes only under the terms of the CC-BY-NC-ND license.
- (2) The integrity of the work and identification of the author, copyright owner, and publisher must be preserved in any copy.
- (3) You must attribute this AAM in the following format: Creative Commons BY-NC-ND license (<http://creativecommons.org/licenses/by-nc-nd/4.0/deed.en>), [+ *Digital Object Identifier link to the published journal article on Elsevier's ScienceDirect® platform*]

Synthesis and preliminary pharmacological characterization of a new class of nitrogen containing bisphosphonates (N-BPs).

Marco L. Lolli,^a Barbara Rolando,^a Paolo Tosco,^a Shilpi Chaurasia,^a Antonella Di Stilo,^a Loretta Lazzarato,^{a,*} Eva Gorassini,^b Riccardo Ferracini,^b Simonetta Oliaro-Bosso,^a Roberta Fruttero^a and Alberto Gasco^a

^a Dipartimento di Scienza e Tecnologia del Farmaco, Università degli Studi di Torino, Via Pietro Giuria 9, 10125 Torino (Italy); ^b CeRMS, Università degli Studi di Torino e ASO San Giovanni Battista, Corso Dogliotti 14, 10126 Torino (Italy)

Abstract: a new series of bisphosphonates bearing either the nitrogen containing NO-donor furoxan (1,2,5-oxadiazole 2-oxide) system or the related furazan (1,2,5-oxadiazole) in lateral chain has been developed. pK_a values and affinity for hydroxyapatite were determined for all the compounds. The products were able to inhibit osteoclastogenesis on RAW 246.7 cells at 10 μ M concentration. The most active compounds were further assayed on human PBMC cells and on rat microsomes. Unlike most nitrogen-containing bisphosphonates which target farnesyl pyrophosphate synthase, experimental and theoretical investigations suggest that the activity of our derivatives may be related to different mechanisms. The furoxan derivatives were also tested for their ability to relax rat aorta strips in view of their potential NO-dependent vasodilator properties.

Keywords

Bisphosphonates, nitric oxide, osteoclastogenesis, cardiovascular diseases.

1. Introduction

* Corresponding author. Tel.: +390116707669; fax: +390116707687; e-mail address: loretta.lazzarato@unito.it

Bisphosphonates (BPs) (**1**, Figure 1) are a class of compounds which contain the P-C-P substructure that, unlike the P-O-P moiety present in pyrophosphate (**2**, Figure 1), is resistant to chemical and enzymatic hydrolysis. They are able to accumulate on the bone mineral surface, as a consequence of their capacity of chelating calcium ions, and, once there, to inhibit bone resorption following internalisation by bone-resorbing osteoclasts (OCs). The affinity to the mineral calcium is increased by the presence of a hydroxy group on the carbon bearing the two phosphonic functions (**1**, R' = OH).¹

The OCs derive from cells of monocyte-macrophage lineage, which fuse to form bone-resorbing cells in the presence of Macrophage Colony Stimulating Factor (M-CSF) and Receptor Activator of Nuclear factor κ B Ligand (RANKL).² A number of BPs are in clinical practice or used in clinical trials for the treatment and prevention of excessive osteoclast-mediated bone resorption typical of certain pathologic states, including Paget's disease, and post-menopausal or glucocorticoid-induced osteoporosis.^{3,4} There is also extensive *in vitro* and *in vivo* preclinical evidence that some BPs, particularly the most potent compounds containing a nitrogen atom in the lateral chain (N-BPs), possess antitumor activity and can reduce skeletal tumor burden and inhibit formation of bone metastases in animal models.⁵ BPs can affect osteoclasts through two different molecular mechanisms.^{3,6} The former, which is typical of products devoid of nitrogen and containing short R and R' side chains (first generation BPs, Figure 1),⁶ is their incorporation into non-hydrolysable ATP analogues. These metabolites accumulate in the cell cytoplasm with consequent inhibition of numerous intracellular metabolic enzymes, resulting in detrimental effects on cell function and survival. The latter, which is typical of second and third generation N-BPs (Figure 1, *N*-aliphatic and *N*-heteroaromatic respectively)⁷ is the blockade of protein prenylation due to their ability to inhibit the mevalonate pathway. The main biochemical target of bisphosphonates is farnesyl pyrophosphate synthase (FPPS), an enzyme of the presqualenic part of the sterol biosynthetic pathway. Some BPs were found to inhibit the conversion of farnesyl pyrophosphate to geranylgeranyl pyrophosphate through the blockade of geranylgeranyl pyrophosphate synthase (GGPPS); the consequent inhibition of protein geranylgeranylation would then lead to apoptotic programmed cell death.⁸ Ibandronate and other derivatives also behave as inhibitors of squalene synthase, although their anti-

resorptive potency does not parallel their degree of inhibition of this enzyme.⁹ Interestingly, BPs have been shown to inhibit atherogenesis.¹⁰ They accumulate extensively in arterial walls where they suppress macrophages in atheromatous lesions, inhibit arterial calcification and lipid accumulation. Recently, great interest is being taken in BPs, also in view of the emerging relationship between osteoporosis and cardiovascular disease (CD).^{11,12}

In this paper we report synthesis, physico-chemical characterisation and pharmacological profile of a new series of N-BPs bearing the nitrogen-containing furoxan (1,2,5-oxadiazole 2-oxide) system or the related furazan (1,2,5-oxadiazole) in the lateral chain. Since it is known that furoxans can produce NO under the action of thiol cofactors,¹³ furoxan bisphosphonates herein described represent a new class of NO-donor bisphosphonates (NO-BPs). The corresponding furazan derivatives were taken as references since they are unable to release NO. NO is involved in the regulation of many physiological processes. In the cardiovascular system it plays important roles in maintaining micro and macrovascular homeostasis through a number of mechanisms including vascular relaxation, inhibition of platelet aggregation and smooth muscle cell proliferation, modulation of monocyte and platelet adhesion.^{14,15} Its impaired production is associated to many forms of CD; among them, atrial fibrillation and atherosclerosis. It is also an essential modulator of gastric mucosal defence.¹⁶ Nitric oxide plays a role in bone remodelling, affecting osteoclast and osteoblast proliferation in a biphasic manner: high concentrations inhibit formation of these bone cells, while low concentrations support their development.¹⁷

Therefore, NO-BPs could represent interesting tools in therapy to limit bone loss and atherogenesis. In addition, they could display reduced gastric irritation¹ and atrial fibrillation risk,¹⁸ two well known drawbacks of BPs.

2. Results and Discussion

2.1 Chemistry

The synthetic route to the target compounds is outlined in Schemes 1-3. Phenylfurazan and phenylfuroxan BPs **12** and **12a** were easily obtained starting from nitrofurazan and nitrofuroxan

derivatives **7** and **7a**, respectively. These products were reacted with tetraethyl 5-hydroxypentylidene bisphosphonate **9** in the presence of $t\text{-BuO}^-\text{K}^+$ to afford intermediate phosphonates **10**, **10a**, which were transformed into the final acids by action of bromotrimethylsilane (TMSBr) and methanol. Similarly, phenylsulfonylfurazan and phenylsulfonylfuroxan BPs **13**, **13a** were obtained starting from bis(phenylsulfonyl) substituted furazan and furoxan **8** and **8a** respectively, through intermediates **11**, **11a** (Scheme 1).

BPs **19**, **19a**, **20**, **20a**, bearing a hydroxyl group on the carbon adjacent to phosphonic functions, were prepared starting from the phenylsulfonyl substituted furazans **8**, **14** and furoxans **8a**, **14a** by nucleophilic displacement of one phenylsulfonyl group under the action of 1,5-pentanediol. This reaction afforded the intermediate alcohols **15**, **15a**, **16**, **16a** which were subsequently oxidised to the related acids **17**, **17a**, **18**, **18a** using Jones reagent. The reaction of these products with thionyl chloride generated the corresponding acylchlorides **A**, which, without further purification, were treated with trimethyl phosphite in dry THF to yield the related acylphosphonates **B** (Michaelis-Arbuzov reaction). The products were immediately transformed into the expected tetramethyl 1-hydroxybisphosphonates **C** by action of dimethylphosphite in dry THF, in the presence of diethylamine. These esters were purified by flash chromatography and immediately transformed into the final BPs under the action of TMSBr and methanol (Scheme 2).

The analogues of alendronate **24**, **24a**, **25**, **25a** bearing furazan and furoxan substructures were prepared from bromomethylsubstituted furazans and furoxans **21**, **21a**, **22**, **22a** by action of *N*-methylalendronate **23** (Scheme 3).

2.2 Dissociation constants

In Table 1 the pK_a values of the final bisphosphonic acids are reported. They were measured by pH-metric method using a Sirius GLpKa instrument. In the case of BPs not bearing an amino nitrogen in the lateral chain, four dissociation constants were detected. This is in keeping with the very low basicity of the furazan and furoxan rings that, in the pH range studied (1.2-12), do not undergo protonation.¹⁹ The pK_{a1} value, corresponding to the first ionization of the bisphosphonic group, is not detectable by this

method because it is too low. All the pK_a values are in keeping with those found for similar compounds.^{20,21} In the case of compounds **24**, **24a**, **25** and **25a** the picture is complicated by the presence of a fifth pK_a associated with the protonation of the basic nitrogen. These pentaprotic BPs have three dissociation constants (pK_{a1} , pK_{a2} , pK_{a5}) corresponding to the first, second, and fourth ionization of the bisphosphonic group. In the physiological pH range there are two ionization steps described by pK_{a3} and pK_{a4} macroconstants that result from overlapping ionizations of the third bisphosphonic group and the amino nitrogen in the lateral chain. To assign pK_a values to these centres we measured the ionization constants in the presence of methanol. The pK_{a3} and pK_{a4} were obtained by the plots of the apparent pK_a values assessed by potentiometric titration in co-solvent mixtures (water/methanol) vs the % methanol (% w/w) in the mixtures. Where straight lines with negative slopes were obtained the value was attributed to the prevalent ionization of the amine substructure of each compound (pK_{a4}). This behaviour is typical of the basic centres.²²

2.3 Hydroxyapatite affinity

BPs are trapped by hydroxyapatite (HAP) calcium present at the sites of new bone formation, giving rise to the formation of stable complexes. After incorporation in the bone they interact with osteoblasts and osteoclasts through a variety of biochemical pathways inducing inhibition of bone resorption. In order to evaluate their affinity for HAP, BPs described in the present work were incubated with HAP, according to a procedure described elsewhere.²³ After 0-h, 6-h and 24-h incubation, the residual concentration of BPs in solution was determined by reverse phase HPLC. The results obtained are collected in Table 1. As expected, ibandronate (**5**), 1-hydroxy-substituted BPs **19**, **19a**, **20**, **20a** and the analogues of alendronate **24**, **24a**, **25** and **25a**, due to their ability to form tridentate complexes with Ca^{2+} , display higher affinity for HAP than their analogues **12**, **12a**, **13**, **13a** deprived of the hydroxy function. These data are in keeping with previous results reported in literature.⁶

2.4 Osteoclastogenesis inhibition

All the compounds were tested for their ability to inhibit osteoclastogenesis on RAW 246.7 cells, a murine monocyte/macrophage cell line with pre-osteoclastic attributes (TIB-71) at 10 μ M concentration, according to the protocol reported in the Experimental Section; the results are collected in Figure 2. All the compounds were able to significantly decrease the number of developed osteoclasts compared to the controls, in a manner not significantly different from ibandronate. Furoxan and related furazan derivatives behave likewise, but a trend of higher activity of the latter compared to the former can be observed. Since the congener furazan derivatives, which are devoid of the capacity to release NO, are endowed with anti-resorptive activity near that of the related furoxans, we have to conclude that in the latter NO does not play crucial roles in their antiosteoclastogenic action, unlike what happens in a series of nitrooxy-substituted BPs we recently developed.¹¹ The most active pairs of products, namely **20**, **20a**, **12**, **12a**, **25**, **25a**, were also tested at 10 μ M concentration on PBMC cells collected from healthy controls (Figure 3). The results are similar to those obtained working with RAW 246.7 cells. The most relevant differences are a slightly higher activity of derivatives **12** and **20a**.

2.5 Enzymatic assays and molecular modelling

One of the main pharmacological targets of BPs is known to be farnesyl pyrophosphate synthase (FPPS);⁴ therefore, the most active compounds of the series (**12**, **12a**, **20**, **20a**) were tested for their ability to inhibit FPPS and other enzymes of the pre-squalene section of sterol biosynthesis, e.g. squalene synthase (SQS). A preliminary test carried out by incubating a rat liver S10 supernatant with labelled (*R,S*)-[2-¹⁴C]-mevalonic acid showed that in the presence of the oxidosqualene cyclase inhibitor U14266A and in the absence of bisphosphonate most radioactivity accumulated into a band co-eluting with squalene. In the presence of bisphosphonates **12**, **20**, **20a** (10 μ M) or ibandronate **5** (1 μ M) the peak of radioactivity co-eluting with squalene completely disappeared, indicating a possible inhibition of one or more enzymes of the pre-squalenic sterol biosynthetic pathway. When tests were repeated with the S100 supernatant, a subcellular fraction deprived of most squalene synthase activity, radioactivity mainly accumulated into a chromatographic fraction corresponding to unresolved metabolites derived from the hydrolysis of prenyl

pyrophosphates. This radioactive fraction diminished by 50% in assays with 1 μ M ibandronate, while a similar effect was not observed with bisphosphonates **12**, **12a**, **20**, **20a**. The decrease of radioactivity in the prenyl intermediates fraction in the presence of ibandronate was in agreement with inhibition of FPPS, a known target of this molecule. The bisphosphonates **12**, **12a**, **20**, **20a**, causing an inhibition of the pre-squalenic biosynthetic pathway following the incubation of (*R,S*)-[2- 14 C]-mevalonic acid in the S10, but not in the S100 cellular fraction, are more likely inhibitors of squalene synthase. The inhibition of squalene synthase by compounds **12**, **12a**, **20**, **20a** and ibandronate was tested by incubating microsomes with the labelled substrate farnesyl pyrophosphate. The values of IC₅₀ are listed in Table 2. Compounds **20** and **20a** are the most active compounds against squalene synthase, showing IC₅₀s of 3.71 ± 0.42 μ M and 7.95 ± 2.23 μ M respectively. Compounds **12** and **12a** have a lower activity, with IC₅₀ ramping around 20 μ M. All bisphosphonates tested are less active than ibandronate (IC₅₀ = 0.64 ± 0.16 μ M), but, from the results obtained with the S100 supernatant, appear to be more specific inhibitors of squalene synthase. On the basis of these assays, it is not possible to rule out a contribution by GGPPS blockade to the antiosteoclastogenic action exerted by compounds **12**, **12a**, **20**, **20a**, since an eventual inhibitory effect on this enzyme would not result in a significant reduction of squalene or isoprenoid metabolites.

In the attempt to rationalise the activity profile of the most active compounds **20**, **20a** compared to ibandronate, a molecular modelling investigation was carried out. Taking advantage of the existence of crystal structures of human FPPS,²⁴ SQS²⁵ and GGPPS,²⁶ flexible docking of the aforementioned bisphosphonates was accomplished in the active site of these three enzymes. In the case of FPPS, since a co-crystal with ibandronate has been obtained,²⁴ we had the opportunity to validate our approach, verifying that AutoDock 4.0 is able to reproduce the crystal pose of the reference inhibitor within the limits of experimental error (RMS deviation on heavy atoms 0.52 Å). Additionally, the pose that reproduces the experimental binding mode also belongs to the most populated cluster, characterized by the best docking score (average $\Delta G_{\text{binding}} = -11.34$ kcal mol⁻¹). Analysing the results for the newly synthesised bisphosphonates **20** and **20a** the situation is radically different (Figure 4a). Respectively, only 7 and 3 poses over 200 are located in the enzyme cavity, with average $\Delta G_{\text{binding}} = -4.48$ and -3.22

kcal mol^{-1} , while in the remaining runs the inhibitor was placed in the bulk water outside the enzyme. This outcome is amenable to the steric bulk of the oxadiazole ring, which hinders these compounds from entering the active site. The presence of the heterocycle at one end of the lipophilic tail also appears to restrict the conformational freedom of the bisphosphonate head, which is not able to establish interactions as effectively as ibandronate does. In particular, each of the phosphonate moieties of ibandronate gives rise to electrostatic interactions with the metal ions present in the active site, in addition to charge-enhanced hydrogen bonds with Arg112, Lys200 and Lys257.²⁴ Instead, in the case of compounds **20** and **20a** the bisphosphonate head is rotated, which results in only one of the phosphonate moieties coming into close contact with metal ions and Lys200, while Arg112 and Lys257 are not within hydrogen-bonding distance. The loss of these interactions sums up to the lack of a protonated nitrogen atom capable of hydrogen bonding with the side chain of Thr201.²⁴ Finally, the phenylsulfonyl substituent on the oxadiazole ring protrudes out of the cavity, as evidenced by the representation of the solvent-excluded surface of the cavity in Figure 4a; the exposure to water of such a hydrophobic moiety further penalizes the binding of these inhibitors. Overall, this picture yields a reasonable interpretation of the lack of affinity for FPPS displayed by compounds **20**, **20a**. The docking results on SQS and GGPPS appear markedly different from the ones on FPPS. While these enzymes share some degree of structural homology, the solvent accessible volume of the FPPS cavity is only about 260 \AA^3 , compared to 608 \AA^3 for GGPPS and 1240 \AA^3 for SQS. These differences are due to the fact that FPPS is designed to catalyse the condensation between dimethyl allyl pyrophosphate (DMAPP) and isopentenyl pyrophosphate (IPP), which are both small substrates. On the contrary, GGPPS needs to accommodate FPP and IPP, while the SQS cavity is even broader to allow the condensation of two FPP molecules. Consequently, both ibandronate and the oxadiazole bisphosphonates are well accommodated in the cavities of SQS and GGPPS. On SQS both ibandronate and newly synthesised BPs display fair docking scores (ibandronate: average $\Delta G_{\text{binding}} = -7.07 \text{ kcal mol}^{-1}$; **20** and **20a**: -8.26 and $-8.21 \text{ kcal mol}^{-1}$, respectively; Figure 4b). The phosphonate heads bind similarly, establishing electrostatic interactions with three arginine residues (Arg52, Arg77 and Arg218), while the lipophilic tails lie in a pocket lined by mostly hydrophobic

residues (Phe72, Tyr73, Leu76, Val179, Leu183, Leu211 and Phe288; Figure 4b). Coming to GGPPS, the ligands' phosphate groups interact with both metal ions present in the active site, as well as with positively charged Arg73, Lys151, Lys202, Lys212. While ibandronate establishes a charge-enhanced hydrogen bond between its protonated nitrogen and the carboxylate group of Asp188, compounds **20** and **20a** stack their phenylsulfonyl substituent between the aromatic side chains of His57, Phe156 and Phe184. All ligands display similar, good *in silico* affinity (ibandronate: average $\Delta G_{\text{binding}} = -11.15 \text{ kcal mol}^{-1}$; **20** and **20a**: -10.84 and $-11.55 \text{ kcal mol}^{-1}$, respectively; Figure 4c). These figures indicate that there is a possibility that binding at GGPPS may contribute to the antiosteoclastogenic effect displayed by **20** and **20a**.

2.6 Vasodilator activity

The NO-BPs **12a**, **13a**, **19a**, **20a**, **24a**, **25a** and ibandronate **5** were tested for their ability to relax rat aorta strips precontracted with phenylephrine, in view of their potential NO-dependent vasodilator properties. All furoxan derivatives were capable of dilating the contracted tissue in a concentration-dependent manner, while ibandronate resulted completely inactive. An example of this behaviour is reported in Figure 5. The vasodilator potencies (EC_{50}) of the products are collected in Table 3. When the experiments were repeated in the presence of $1 \mu\text{M}$ ODQ (1*H*-[1,2,4]oxadiazolo[4,3-*a*]quinoxalin-1-one), a strong decrease in potency was observed, in keeping with a NO-mediated, sGC-dependent vasodilator mechanism. The potencies of these hybrids parallel the ones of the simple reference furoxan models,²⁷ while being consistently lower. This is most likely due to the highly hydrophilic character of NO-BPs, which reduces their capacity to enter into vascular smooth muscle cells where they are metabolised to NO.

3. Conclusion

A new series of bisphosphonates bearing either the nitrogen-containing NO-donor furoxan (1,2,5-oxadiazole 2-oxide) or the related furazan (1,2,5-oxadiazole) systems in the lateral chain has been developed. Their pK_a profile is in keeping with that of similar compounds. As expected, 1-hydroxy

substituted products show a higher affinity for HAP than their methylene analogues. All the new BPs are able to inhibit osteoclastogenesis on RAW 246.7 and PBMC cells at 10 μ M concentration. The most active compounds were tested for their ability to inhibit the mevalonate pathway. The assay indicates that they are more potent inhibitors of SQS compared to FPPS, while an involvement of other targets (e.g., GGPPS) cannot be ruled out. This finding is in keeping with the results of a molecular modelling investigation, but additional experimental work is necessary to draw definitive conclusions on the mechanism of action. NO-BPs are able to relax contracted vascular tissue in a concentration-dependent manner. A decrease in potency was observed in the presence of ODQ, proving the involvement of NO in the vasodilator mechanism. This new series of NO-BPs is worthy of additional studies as potential drugs in view of the emerging relationship between osteoporosis and CD.

4. Experimental Section

4.1 Chemistry

^1H and ^{13}C -NMR spectra were recorded on a Bruker AC-200 and on a Bruker Avance 300; abbreviations: s, singlet; d, doublet; t, triplet; tt, triplet of triplets; m, multiplet; br, broad; Fx, furoxan; Fz, furazan. Low resolution mass spectra were recorded with a Finnigan-Mat TSQ-700. Melting points were determined with a capillary apparatus (Büchi 540). Flash column chromatography was performed on silica gel (Merck Kieselgel 60, 230-400 mesh ASTM); PE stands for 40-60 petroleum ether. The progress of the reactions was followed by thin layer chromatography (TLC) on 5×20 cm plates with a layer thickness of 0.25 mm. Anhydrous magnesium sulfate was used as the drying agent for the organic phases. Organic solvents were removed under vacuum at 30 $^{\circ}\text{C}$. Preparative HPLC was performed on a Lichrospher[®] C₁₈ column (250×25 mm, 10 μ m) (Merck Darmstadt, Germany) with a Varian ProStar mod-210 with Varian UV detector mod-325. When necessary they were developed with iodine, KMnO_4 and ammonium thiocyanate-iron(III) chloride reagent.²⁸ Elemental analyses (C, H, N) were performed by REDOX (Monza) and the results are within 0.4% of the theoretical values. Compounds **7**,²⁹ **7a**,²⁹ **8**,³⁰ **8a**,³¹ **9**,²¹

14,²⁹ **14a**,²⁹ **21**,³² **21a**,³³ **22**,³² **22a**,³⁴ **23**³³ were synthesised according to literature. Tetrahydrofuran (THF) was distilled immediately before use from Na and benzophenone under a positive atmosphere of N₂.

4.1.1 General procedure for the preparation of esters **10**, **10a**, **11**, **11a**

A solution of potassium tert-butyrate (0.416 M; 11 mL; 4.58 mmol) in dry THF was added over 90 min to a solution of **9** (1.50 g; 4.16 mmol) and the appropriate furazan (**7**, **8**) or furoxan (**7a**, **8a**) (4.58 mmol) in dry THF (15 mL), stirred under inert atmosphere between -45 and -15 °C. The mixture was allowed to reach room temperature, then diluted with saturated NH₄Cl (20 mL) and extracted with Et₂O (25 mL). The organic phases were collected, washed with saturated NH₄Cl (10 mL), dried and concentrated under reduced pressure. The crude product was purified by flash chromatography using the appropriate eluent obtaining the desired compound as pale yellow oil.

4.1.1.1 Tetraethyl (5-(4-phenylfurazan-3-yloxy)pentylidene) bisphosphonate (10). Eluent from CH₂Cl₂ to CH₂Cl₂/MeOH 98/2 v/v; pale yellow oil; 86% yield. ¹H NMR (200 MHz, CDCl₃, TMS): δ = 1.27-1.37 (m, 12H, -PO(OCH₂CH₃)₂), 1.72-2.17 (m, 6H, -CH₂CH₂CH₂CH-), 2.29 (tt, 1H, ³J_{HH} = 5.8 Hz, ²J_{PH} = 24.0 Hz, -CH₂CH[PO(OCH₂CH₃)₂]₂), 4.07-4.23 (m, 8H, -PO(OCH₂CH₃)₂), 4.46 (t, 2H, ³J_{HH} = 6.6 Hz, -OCH₂-), 7.44-8.00 ppm (m, 5H, C₆H₅); ¹³C NMR (50 MHz, CDCl₃, TMS): δ = 16.2 (d), 25.2 (t), 28.5, 36.6 (t, ¹J_{PC} = 133 Hz), 62.4 (m), 72.3, 125.1, 127.2, 128.8, 130.4, 145.0, 163.4 ppm. MS *m/z* 505 (M+H)⁺. Anal. calcd for C₂₁H₃₄N₂O₈P₂ · 0.5H₂O: C 49.12%, H 6.87%, N 5.46%, found: C 48.92%, H 6.99%, N 5.34%.

4.1.1.2 Tetraethyl (5-(3-phenylfuroxan-4-yloxy)pentylidene) bisphosphonate (10a). Eluent: from CH₂Cl₂ to CH₂Cl₂/MeOH 98/2 v/v; pale yellow oil; 60% yield. ¹H NMR (200 MHz, CDCl₃, TMS): δ = 1.27-1.36 (m, 12H, -PO(OCH₂CH₃)₂), 1.81-2.02 (m, 6H, -CH₂CH₂CH₂CH-), 2.31 (tt, 1H, ³J_{HH} = 5.8 Hz, ²J_{PH} = 23.8 Hz, -CH₂CH[PO(OCH₂CH₃)₂]₂), 4.52 (t, 2H, ³J_{HH} = 6.1 Hz, -OCH₂-), 4.09-4.25 (m, 8H, -PO(OCH₂CH₃)₂), 7.46-8.16 ppm (m, 5H, C₆H₅); ¹³C NMR (50 MHz, CDCl₃, TMS): δ = 16.2 (d), 25.2 (t), 28.3, 36.6 (t, ¹J_{PC} = 133 Hz), 62.4 (t), 70.3, 107.4, 122.4, 126.0, 128.7, 130.3, 162.2 ppm. MS *m/z*

521 (M+H)⁺. Anal. calcd for C₂₁H₃₄N₂O₉P₂: C 48.46%, H 6.58%, N 5.38%, found: C 48.53%, H 6.73%, N 5.27%.

4.1.1.3 Tetraethyl (5-(4-phenylsulfonylfurazan-3-yloxy)pentylidene) bisphosphonate (11). Eluent: CH₂Cl₂/MeOH 98/2 v/v; pale yellow oil; 58% yield. ¹H NMR (200 MHz, CDCl₃, TMS): δ = 1.31-1.38 (m, 12H, -PO(OCH₂CH₃)₂), 1.67-2.13 (m, 6H, -CH₂CH₂CH₂CH-), 2.28 (tt, 1H, ³J_{HH} = 5.8 Hz, ²J_{PH} = 24.0 Hz, -CH₂CH[PO(OCH₂CH₃)₂]₂), 4.11-4.27 (m, 8H, -PO(OCH₂CH₃)₂), 4.37 (t, 2H, ³J_{HH} = 6.2 Hz, -OCH₂-), 7.60-8.12 ppm (m, 5H, C₆H₅); ¹³C NMR (50 MHz, CDCl₃, TMS): δ = 16.3 (d), 25.0 (t), 28.2, 36.5 (t, ¹J_{PC} = 143 Hz), 62.4 (t), 73.3, 128.8, 129.5, 135.3, 137.7, 148.0, 161.1 ppm. MS *m/z* 569 (M+H)⁺. Anal. calcd for C₂₁H₃₄N₂O₁₀P₂S: C 44.37%, H 6.03%, N 4.93%, found: C 44.47%, H 6.11%, N 4.87%.

4.1.1.4 Tetraethyl (5-(3-phenylsulfonylfuroxan-4-yloxy)pentylidene) bisphosphonate (11a). Eluent: CH₂Cl₂/MeOH 98/2 v/v; pale yellow oil; 59% yield. ¹H NMR (200 MHz, CDCl₃, TMS): δ = 1.35-1.45 (m, 12H, -PO(OCH₂CH₃)₂), 1.80-2.00 (m, 6H, -CH₂CH₂CH₂CH-), 2.30 (tt, 1H, ³J_{HH} = 5.8 Hz, ²J_{PH} = 24.0 Hz, -CH₂CH[PO(OCH₂CH₃)₂]₂), 4.12-4.28 (m, 8H, -PO(OCH₂CH₃)₂), 4.43 (t, 2H, ³J_{HH} = 6.0 Hz, -OCH₂-), 7.60-8.09 ppm (m, 5H, C₆H₅); ¹³C NMR (50 MHz, CDCl₃, TMS): δ = 16.3 (d), 25.0 (t), 26.1, 36.5 (t, ¹J_{PC} = 132 Hz), 62.4 (t), 71.0, 110.3, 137.9, 128.4, 129.5, 135.4, 158.8 ppm. MS *m/z* 585 (M+H)⁺. Anal. calcd for C₂₁H₃₄N₂O₁₁P₂S: C 43.15%, H 5.86%, N 4.79%, found: C 43.36%, H 6.03%, N 4.68%.

4.1.2 General procedure for the preparation of acids 12, 12a, 13, 13a

Bromotrimethylsilane (2.30 mL; 17.6 mmol; 10 eq) was added over 15 min to a solution of the appropriate ester (**10**, **10a**, **11**, **11a**) (1.76 mmol) in dry CH₂Cl₂ (10 mL) under inert atmosphere. The mixture was stirred at room temperature for 3.5 h, then ice cooled and slowly diluted with MeOH (15 mL). The resulting mixture was stirred at room temperature for 30 min, then concentrated under reduced pressure. After dissolving the crude product in MeOH (15 mL), the resulting solution was concentrated

under reduced pressure three times. The crude product was then dissolved in CH₃CN (2 mL); the resulting solution was diluted with water (8 mL) and the mixture was purified by flash RP-18 chromatography (eluent CH₃CN/H₂O 2/8 v/v) obtaining a foamy solid. The desired compound was obtained as a white solid triturating with dry Et₂O.

4.1.2.1 5-(4-Phenylfurazan-3-yloxy)pentylidenebis(phosphonic)acid (12). White solid; 82% yield. ¹H NMR (200 MHz, DMSO-*d*₆, TMS): δ = 1.60-2.20 (m, 7H, -CH₂CH₂CH₂CH-), 4.42-4.44 (m, 2H, -OCH₂-), 7.58-7.98 (m, 5H, C₆H₅), 8.57 ppm (br s, 4H, mobile protons); ¹³C NMR (50 MHz, DMSO-*d*₆, TMS; a signal is missing, being covered by the solvent): δ = 24.9, 28.2, 72.8, 124.5, 127.4, 129.5, 131.1, 145.3, 163.4 ppm; ³¹P NMR (120 MHz, D₂O, H₃PO₄): δ = 23.4 ppm. Anal. calcd for C₁₃H₁₈N₂O₈P₂ · 0.15H₂O: C 39.53%, H 4.67%, N 7.09%, found: C 39.17%, H 4.7%, N 7.03%.

4.1.2.2 5-(3-Phenylfuroxan-4-yloxy)pentylidenebis(phosphonic)acid (12a). White solid; 67% yield. ¹H NMR (200 MHz, DMSO-*d*₆, TMS): δ = 1.60-2.20 (m, 7H, CH₂CH₂CH₂CH-), 4.48 (m, 2H, -OCH₂-), 7.56-8.08 (m, 5H, C₆H₅), 9.48 ppm (br s, 4H, mobile protons); ¹³C NMR (50 MHz, DMSO-*d*₆, TMS; a signal is missing, being covered by the solvent): δ = 24.9, 28.0, 71.7, 107.6, 122.1, 123.3, 129.2, 130.7, 162.4 ppm; ³¹P NMR (120 MHz, D₂O, H₃PO₄): δ = 23.8 ppm. Anal. calcd for C₁₃H₁₈N₂O₉P₂: C 38.25%, H 4.44%, N 6.86%, found: C 38.28%, H 4.48%, N 6.85%.

4.1.2.3 5-(4-Phenylsulfonylfurazan-3-yloxy)pentylidenebis(phosphonic) acid (13). White solid, 55% yield. ¹H NMR (200 MHz, DMSO-*d*₆, TMS): δ = 1.40-2.10 (m, 7H, -CH₂CH₂CH₂CH-), 4.33-4.36 (m, 2H, -OCH₂-), 7.76-8.12 (m, 5H, C₆H₅), 9.88 ppm (br s, 4H, mobile protons); ¹³C NMR (50 MHz, DMSO-*d*₆, TMS, a signal is missing, being covered by the solvent): δ = 24.0, 28.8, 74.0, 128.8, 130.3, 136.3, 136.8, 148.8, 161.0 ppm; ³¹P NMR (120 MHz, D₂O, H₃PO₄): δ = 22.7 ppm. Anal. calcd for C₁₃H₁₈N₂O₁₀P₂S: C 34.22%, H 3.98%, N 6.14%, found: C 34.17%, H 3.98%, N 6.11%.

4.1.2.4 5-(3-Phenylsulfonylfuroxan-4-yloxy)pentylidenebis(phosphonic) acid (13a). White solid; 77% yield. ^1H NMR (200 MHz, DMSO- d_6 , TMS): δ = 1.50-2.20 (m, 7H, $-\text{CH}_2\text{CH}_2\text{CH}_2\text{CH}-$), 4.38 (m, 2H, $-\text{OCH}_2-$), 7.74-8.06 (m, 5H, C_6H_5), 8.31 ppm (br s, 4H, mobile protons); ^{13}C NMR (50 MHz, DMSO- d_6 , TMS, a signal is missing, being covered by the solvent): δ = 24.7, 27.9, 71.3, 110.6, 128.5, 130.2, 136.2, 137.2, 158.9 ppm; ^{31}P NMR (120 MHz, D_2O , H_3PO_4): δ = 23.4 ppm. Anal. calcd for $\text{C}_{13}\text{H}_{18}\text{N}_2\text{O}_{11}\text{P}_2\text{S}$: C 33.06%, H 3.84%, N 5.93%, found: C 32.79%, H 4.01%, N 5.80%.

4.1.3 General procedure for the preparation of alcohols 15, 15a, 16, 16a

NaOH (50% w/w; 1.5 eq) was added over a period of 30 min to a stirred solution of the appropriate phenylsulfonyl derivative (**8**, **8a**, **14**, **14a**) (8.0 g) and 1,5-pentanediol (10 eq) in distilled THF (100 mL). Acetic acid was added to the mixture that was concentrated under reduced pressure. The residue was dissolved in EtOAc (100 mL) and washed twice with H_2O (100 mL). The organic layer was dried and concentrated under reduced pressure. The crude product was purified by flash chromatography to give the pure product as a white solid.

4.1.3.1 5-(4-Phenylfuroxan-3-yloxy)pentan-1-ol (15). Eluent: PE/EtOAc from 80/20 to 60/40 v/v, white solid, 86% yield; mp 59-60 °C (*i*Pr $_2$ O). ^1H NMR (300 MHz, CDCl_3 , TMS): δ = 1.34 (s, 1H, OH), 1.50-1.70 (m, 4H), 1.88-1.97 (m, 2H)($-\text{OCH}_2\text{CH}_2\text{CH}_2\text{CH}_2\text{CH}_2\text{OH}$), 3.66 (t, 2H, $^3J_{\text{HH}} = 6.0$ Hz, $-\text{CH}_2\text{OH}$), 4.44 (t, 2H, $^3J_{\text{HH}} = 6.6$ Hz, $-\text{FzOCH}_2-$), 7.44-7.48 (m, 3H, C_6H_5), 7.93-7.97 ppm (m, 2H, C_6H_5); ^{13}C NMR (75 MHz, CDCl_3 , TMS): δ = 22.1, 28.6, 32.2, 62.6, 72.8, 125.3, 127.4, 129.0, 130.6, 145.2, 163.6 ppm. MS m/z 249 ($\text{M}+\text{H}$) $^+$. Anal. calcd for $\text{C}_{13}\text{H}_{16}\text{N}_2\text{O}_3$: C 62.89%, H 6.50%, N 11.28%, found: C 62.50%, H 6.47%, N 11.19%.

4.1.3.2 5-(3-Phenylfuroxan-4-yloxy)pentan-1-ol (15a). Eluent: PE/EtOAc 80/20 v/v, white solid, 98% yield; mp 91-92 °C (*i*Pr $_2$ O). ^1H NMR (300 MHz, CDCl_3 , TMS): δ = 1.31 (s, 1H; $-\text{OH}$), 1.54-1.73 (m, 4H), 1.93-2.02 (m, 2H)($-\text{OCH}_2\text{CH}_2\text{CH}_2\text{CH}_2\text{CH}_2\text{OH}$), 3.70 (t, 2H, $^3J_{\text{HH}} = 6.0$ Hz, $-\text{CH}_2\text{OH}$), 4.52 (t, 2H, $^3J_{\text{HH}} = 6.6$ Hz, $-\text{FxOCH}_2-$), 7.44-7.54 (m, 3H, C_6H_5), 8.12-8.15 ppm (m, 2H, C_6H_5); ^{13}C NMR (75

MHz, CDCl₃, TMS): δ = 22.2, 28.5, 32.1, 62.6, 70.8, 107.6, 122.5, 126.2, 128.9, 130.4, 162.4 ppm. MS m/z 265 (M+H)⁺. Anal. calcd for C₁₃H₁₆N₂O₄: C 59.08%, H 6.10%, N 10.60%, found: C 58.98%, H 6.07%, N 10.57%.

4.1.3.3 5-(4-Phenylsulfonylfurazan-3-yloxy)pentan-1-ol (16). Eluent: PE/EtOAc 60/40 v/v, colourless oil, 57% yield. ¹H NMR (300 MHz, CDCl₃, TMS): δ = 1.39-1.61 (m, 5H), 1.76-1.85 (m, 2H)(-OCH₂CH₂CH₂CH₂CH₂OH), 3.61 (t, 2H, ³J_{HH} = 6.2 Hz, -CH₂OH), 4.31 (t, 2H, ³J_{HH} = 6.4 Hz, -FzOCH₂-), 7.54-7.59 (t, 2H, C₆H₅), 7.67-7.72 (t, 1H, C₆H₅), 8.00-8.03 ppm (d, 2H, C₆H₅); ¹³C NMR (75 MHz, CDCl₃, TMS): δ = 21.7, 28.0, 31.8, 62.2, 73.6, 128.7, 129.4, 135.2, 137.5, 148.6, 161.1 ppm. MS m/z 313 (M+H)⁺. Anal. calcd for C₁₃H₁₆N₂O₅S: C 49.99%, H 5.16%, N 8.97%, found: C 49.72%, H 5.25%, N 9.00%.

4.1.3.4 5-(3-Phenylsulfonylfuroxan-4-yloxy)pentan-1-ol (16a). Eluent: PE/EtOAc 50/50 v/v, white solid, 59% yield; mp 72 °C (*i*Pr₂O). ¹H NMR (200 MHz, CDCl₃): δ = 1.42 (br s, 1H, -OH), 1.49-2.00 (m, 6H, -OCH₂CH₂CH₂CH₂CH₂OH), 3.69-3.74 (m, 2H, -CH₂OH), 4.45 (t, 2H, ³J_{HH} = 6.3 Hz, -FxOCH₂-), 7.60-7.81 (m, 3H, C₆H₅), 8.07 ppm (d, 2H, C₆H₅); ¹³C NMR (50 MHz, CDCl₃): δ = 21.7, 27.9, 31.8, 62.3, 71.2, 110.2, 128.3, 129.4, 135.4, 137.8, 158.8 ppm. MS m/z 329 (M+H)⁺. Anal. calcd for C₁₃H₁₆N₂O₆S · 0.25H₂O: C 46.91%, H 5.00%, N 8.42%, found: C 47.03%, H 4.80%, N 8.41%.

4.1.4 General procedure for the preparation of carboxylic acids 17, 17a, 18, 18a

A solution of Jones reagent (2.5 M, 2.5 eq) was added to a stirred solution of the appropriate alcohol (**15**, **15a**, **16**, **16a**) (5.0 g) in acetone (100 mL), cooled at 0 °C. The mixture was allowed to reach room temperature and then stirred for 18 h. *i*PrOH (20 mL) was added, then the mixture was concentrated under reduced pressure. The residue was dissolved in Et₂O (100 mL), washed with H₂O (3 × 100 mL) and then extracted with a saturated solution of NaHCO₃ (4 × 30 mL). The aqueous layers were acidified with 6 M HCl and extracted with Et₂O (3 × 100 mL). The combined organic layers were dried, filtered and concentrated under reduced pressure to give the pure compound as a white solid.

4.1.4.1 5-(4-Phenylfurazan-3-yloxy)pentanoic acid (17). 72% yield; mp 85.5-87.5 °C (*i*Pr₂O). ¹H NMR (300 MHz, CDCl₃, TMS): δ = 1.86-2.00 (m, 4H, -OCH₂CH₂CH₂CH₂COOH), 2.49 (t, 2H, ³J_{HH} = 7.2 Hz, -OCH₂CH₂CH₂CH₂COOH), 4.48 (t, 2H, ³J_{HH} = 6.0 Hz, -FzOCH₂-), 7.47-7.50 (m, 3H, C₆H₅), 7.97-8.00 (m, 2H, C₆H₅), 11.55 ppm (br s, 1H, COOH); ¹³C NMR (75 MHz, CDCl₃, TMS): δ = 21.0, 28.2, 33.4, 72.2, 125.2, 127.4, 129.0, 130.7, 145.2, 163.6, 179.3 ppm. MS *m/z* 263 (M+H)⁺. Anal. calcd for C₁₃H₁₄N₂O₄: C 59.54%, H 5.38%, N 10.68%, found: C 59.31%, H 5.37%, N 10.58%.

4.1.4.2 5-(3-Phenylfuroxan-4-yloxy)pentanoic acid (17a). 76% yield; mp 113.5-114.5 °C (*i*Pr₂O). ¹H NMR (300 MHz, CDCl₃, TMS): δ = 1.84-2.05 (m, 4H, -OCH₂CH₂CH₂CH₂COOH), 2.49 (t, 2H, ³J_{HH} = 7.2 Hz, -OCH₂CH₂CH₂CH₂COOH), 4.52 (t, 2H, ³J_{HH} = 6.3 Hz, -FxOCH₂-), 7.44-7.54 (m, 3H, C₆H₅), 8.10-8.17 (m, 2H, C₆H₅), 11.48 ppm (br s, 1H, COOH); ¹³C NMR (75 MHz, CDCl₃, TMS): δ = 21.0, 28.0, 33.3, 70.3, 107.6, 122.4, 126.2, 128.9, 130.5, 162.3, 179.2 ppm. MS *m/z* 279 (M+H)⁺. Anal. calcd for C₁₃H₁₄N₂O₅: C 56.11%, H 5.07%, N 10.07%, found: C 56.10%, H 5.11%, N 10.03%.

4.1.4.3 5-(4-Phenylsulfonylfurazan-3-yloxy)pentanoic acid (18). 65% yield; mp 96-97 °C (*i*Pr₂O). ¹H NMR (200 MHz, CDCl₃): δ = 1.74-2.00 (m, 4H, -OCH₂CH₂CH₂CH₂COOH), 2.47 (t, 2H, ³J_{HH} = 7.1 Hz, -OCH₂CH₂CH₂CH₂COOH), 4.41 (t, 2H, ³J_{HH} = 5.8 Hz, -FzOCH₂-), 7.60-7.81 (m, 3H, C₆H₅), 8.11 ppm (d, 2H, C₆H₅); ¹³C NMR (50 MHz, CDCl₃): δ = 20.7, 27.7, 33.1, 73.2, 128.6, 129.5, 135.3, 137.6, 146.6, 161.1, 177.0 ppm. MS *m/z* 327 (M+H)⁺. Anal. calcd for C₁₃H₁₄N₂O₆S: C 47.85%, H 4.32%, N 8.58%, found: C 47.63%, H 4.29%, N 8.50%.

4.1.4.4 5-(3-Phenylsulfonylfuroxan-4-yloxy)pentanoic acid (18a). 70% yield; mp 117-120 °C (*i*Pr₂O). ¹H NMR (200 MHz, CDCl₃): δ = 1.79-2.04 (m, 4H, -OCH₂CH₂CH₂CH₂COOH), 2.50 (t, 2H, ³J_{HH} = 7.1 Hz, -OCH₂CH₂CH₂CH₂COOH), 4.45 (t, 2H, ³J_{HH} = 5.8 Hz, -FxOCH₂-), 7.58-7.81 (m, 3H, C₆H₅), 8.06 ppm (d, 2H, C₆H₅); ¹³C NMR (50 MHz, CDCl₃): δ = 20.6, 27.5, 33.1, 70.7, 110.2, 128.3, 129.5, 135.4, 137.8, 158.7, 179.2 ppm. MS *m/z* 343 (M+H)⁺. Anal. calcd for C₁₃H₁₄N₂O₇S: C 45.61%, H 4.12%, N 8.18%, found: C 45.96%, H 4.14%, N 8.13%.

4.1.5 General procedure for the preparation of bisphosphonic acids 19, 19a, 20, 20a

A solution of the appropriate carboxylic acid (**17**, **17a**, **18**, **18a**) (1.0 g) in thionyl chloride (10 mL, fresh distilled) was stirred at room temperature for 3 h under N₂. Thionyl chloride was then distilled under reduced pressure, and the system was refilled with N₂. Thereafter, dry THF (10 mL) was added to the residue and then distilled under reduced pressure three times. The residue was dissolved in dry THF (10 mL) and to the resulting solution, stirred under N₂ at 0 °C, was added trimethylphosphite (1 eq). The mixture was then allowed to reach room temperature and stirred for 18 h. The reaction mixture containing the acylphosphonate (B) was slowly added to a stirred solution of dimethylphosphite (2 eq) and diethylamine (0.4 eq) in dry THF (20 mL) under N₂ and kept at 0 °C. The mixture was stirred at 0 °C for 3 h, allowed to reach room temperature, and then poured into 0.5 M HCl (20 mL) and Et₂O (30 mL). The ethereal fraction was extracted with 0.5 M HCl (25 × 20 mL). The collected aqueous layers were extracted with CH₂Cl₂ (10 × 50 mL). The organic layers were dried and concentrated under reduced pressure. The crude product was purified by flash chromatography (CH₂Cl₂/MeOH 98/2 v/v to 9/1 v/v) to yield the unstable tetramethylester (C) as pale yellow oil. The compounds were immediately used for the next synthetic step. Bromotrimethylsilane (2.5 eq) was slowly added to a solution of the appropriate tetramethylester (C) (0.70 g) in dry CH₂Cl₂ (20 mL), then stirred under inert atmosphere for 48 h. The reaction was followed via RP-18 TLC (CH₃CN/H₂O 5/5 v/v). The solution was cooled at 0 °C, then dry MeOH (10 mL) was added and the mixture was allowed to reach room temperature. The solution was then concentrated under reduced pressure. The residue was dissolved in dry MeOH (10 mL) and concentrated under reduced pressure twice. The crude material was purified by preparative HPLC (Lichrospher 250 × 25 C18, MeOH/H₂O 3/7 v/v, flow rate 39 mL min⁻¹, λ 224 nm, injection volume 2 mL) to give the desired product as a white solid.

4.1.5.1 (5-(4-Phenylfurazan-3-yloxy)-1-hydroxypentylidene)bis(phosphonic)acid (19). 15% yield. ¹H NMR (300 MHz, D₂O): δ = 1.60 (br s, 4H, -OCH₂CH₂CH₂CH₂-), 1.80-2.00 (m, 2H, -OCH₂CH₂CH₂CH₂-), 4.05 (br s, 2H, -FzOCH₂-), 7.07-7.15 (m, 3H, C₆H₅), 7.46-7.48 ppm (m, 2H, C₆H₅); ¹³C NMR (75 MHz,

D₂O): δ = 19.8 (t, $^2J_{\text{PC}}$ = 6.0 Hz), 29.0, 33.6, 72.9, 73.6 (t, $^1J_{\text{PC}}$ = 146 Hz), 124.3, 127.1, 129.0, 130.9, 145.3, 163.4 ppm; ^{31}P NMR (120 MHz, D₂O, H₃PO₄): δ = 20.3 ppm. Anal. calcd for C₁₃H₁₈N₂O₉P₂ · 1.5 H₂O: C 35.87%, H 4.86%, N 6.44%, found: C 35.99%, H 4.73%, N 6.44%.

4.1.5.2 (5-(3-Phenylfuroxan-4-yloxy)-1-hydroxypentylidene)bis(phosphonic)acid (19a) 31% yield. ^1H NMR (300 MHz, D₂O): δ = 1.78-2.04 (m, 6H, -OCH₂CH₂CH₂CH₂-), 4.49 (t, 2H, $^3J_{\text{HH}}$ = 6.9 Hz, -F_xOCH₂-), 7.54-7.56 (m, 3H, C₆H₅), 7.99-8.00 ppm (m, 2H, C₆H₅); ^{13}C NMR (75 MHz, D₂O): δ = 20.7 (t, $^2J_{\text{PC}}$ = 5.5 Hz), 29.6, 36.1, 72.2, 76.8 (t, $^1J_{\text{PC}}$ = 134.0 Hz), 110.3, 121.7, 126.7, 129.2, 131.4, 163.0 ppm; ^{31}P NMR (120 MHz, D₂O, H₃PO₄): δ = 20.4 ppm. Anal. calcd for C₁₃H₁₈N₂O₁₀P₂ · 2.0 H₂O: C 33.92%, H 4.82%, N 6.09%, found: C 33.93%, H 4.56%, N 6.04%.

4.1.5.3 (5-(4-Phenylsulfonylfurazan-3-yloxy)-1-hydroxypentylidene)bis(phosphonic)acid (20). 25% yield. ^1H NMR (200 MHz, D₂O): δ = 1.70-1.88 (m, 4H), 1.98-2.12 (m, 2H, -OCH₂CH₂CH₂CH₂-), 4.35 (t, 2H, $^3J_{\text{HH}}$ = 6.0 Hz, -F_zOCH₂-), 7.70 (t, 2H, C₆H₅), 7.83 (t, 1H, C₆H₅), 8.06 ppm (d, 2H, C₆H₅); ^{13}C NMR (50 MHz, D₂O): δ = 17.0, 26.0, 30.5, 70.6 (t, $^1J_{\text{PC}}$ = 143.0 Hz), 71.4, 126.1, 127.4, 133.1, 133.7, 145.7, 158.6 ppm; ^{31}P NMR (80 MHz, D₂O, H₃PO₄): δ = 20.3 ppm. Anal. calcd for C₁₃H₁₈N₂O₁₁P₂S · 0.75 H₂O: C 32.14%, H 4.04%, N 5.77%, found: C 31.78%, H 4.09%, N 5.66%.

4.1.5.4 (5-(3-Phenylsulfonylfuroxan-4-yloxy)-1-hydroxypentylidene)bis(phosphonic)acid (20a). 30% yield. ^1H NMR (200 MHz, D₂O): δ = 1.71-2.05 (m, 6H, -OCH₂CH₂CH₂CH₂-), 4.34 (t, 2H, $^3J_{\text{HH}}$ = 5.6 Hz, -F_xOCH₂-), 7.55-7.78 (m, 3H, C₆H₅), 7.95 ppm (d, 2H, C₆H₅); ^{13}C NMR (50 MHz, D₂O): δ = 17.2, 25.9, 30.4, 69.1, 70.7 (t, $^1J_{\text{PC}}$ = 141.0 Hz), 108.5, 125.8, 127.3, 133.5, 133.8, 156.7 ppm; ^{31}P NMR (80 MHz, D₂O, H₃PO₄): δ = 20.2 ppm. Anal. calcd for C₁₃H₁₈N₂O₁₂P₂S · 2.5 H₂O: C 29.28%, H 4.35%, N 5.25%, found: C 29.18%, H 4.09%, N 5.07%.

4.1.6 General procedure for the preparation of bisphosphonic acids 24, 24a, 25, 25a

The pH of a solution of **23** (0.36 g; 1.38 mmol) in water (4 mL) was adjusted to 12 by slowly adding 2 M NaOH, then a solution of the appropriate bromomethyl-derivative (**21**, **21a**, **22**, **22a**) (0.9 eq) in CH₃CN (4 mL) was added. The mixture was stirred at room temperature maintaining the pH at 12 by addition of 2 M NaOH. Subsequently, phenylsulfonyl chloride (1 eq) was added, the mixture was stirred at pH 12 until a clear solution was obtained, then pH was adjusted to 8 with 1 M HCl. The mixture was washed with CH₂Cl₂ (3 × 10 mL), then concentrated under reduced pressure. The residue (10 mL) was percolated through Dowex 50W-X8 (200-400 mesh hydrogen form; 20 mL resin bed, 34 meq) eluting with water until neutrality of the eluate. The eluate was concentrated under reduced pressure to obtain the desired compound as a white solid.

4.1.6.1 [4-(*N*-Methyl-*N*-[(4-methylfuran-3-yl)methyl]-1-hydroxybutylidene)bis(phosphonic)acid (24**).** 36% yield; mp 138 °C. ¹H NMR (200 MHz, D₂O): δ = 1.74-2.14 (m, 4H, -CH₂CH₂C(OH)[PO(OH)₂]₂), 2.30 (s, 3H, FzCH₃), 2.87 (s, 3H, -CH₂N(CH₃)CH₂CH₂-), 3.09-3.37 (m, 2H, -CH₂N(CH₃)CH₂CH₂-), 4.52 ppm (s, 2H, -CH₂N(CH₃)CH₂CH₂-); ¹³C NMR (50 MHz, D₂O): δ = 4.54, 16.5 (t, ²J_{PC} = 6.3 Hz), 27.5, 37.8, 44.9, 54.4, 70.1 (t, ¹J_{PC} = 140.0 Hz), 144.6, 148.5 ppm. Anal. calcd for C₉H₁₉N₃O₈P₂ · 1.1 H₂O: C 28.52%, H 5.64%, N 11.07%, found: C 28.17%, H 5.40%, N 10.88%.

4.1.6.2 [4-(*N*-Methyl-*N*-[(3-methylfuroxan-4-yl)methyl]-1-hydroxybutylidene)bis(phosphonic)acid (24a**).** 71% yield; mp 214 °C dec. ¹H NMR (200 MHz, D₂O): δ = 1.70-2.07 (m, 4H, -CH₂CH₂C(OH)[PO(OH)₂]₂), 2.07 (s, 3H, FxCH₃), 2.87 (s, 3H, -CH₂N(CH₃)CH₂CH₂-), 3.06-3.41 (m, 2H, -CH₂N(CH₃)CH₂CH₂-), 4.45 ppm (s, 2H, -CH₂N(CH₃)CH₂CH₂-); ¹³C NMR (50 MHz, D₂O): δ = 4.39, 16.5 (t, ²J_{PC} = 6.8), 27.5, 37.9, 46.2, 54.4, 70.2 (t, ¹J_{PC} = 140.0 Hz), 113.3, 148.0 ppm. Anal. calcd for C₉H₁₉N₃O₉P₂ · 1.5 H₂O: C 26.87%, H 5.51%, N 10.45%, found: C 26.54%, H 5.30%, N 10.17%.

4.1.6.3

[4-(*N*-Methyl-*N*-[(4-carbamoylfuran-3-yl)methyl]-1-hydroxybutylidene)bis(phosphonic)acid (25**).** 34% yield. ¹H NMR (200 MHz, D₂O): δ = 1.76-2.18 (m, 4H, -CH₂CH₂C(OH)[PO(OH)₂]₂), 2.89 (s,

3H, $-\text{CH}_2\text{N}(\text{CH}_3)\text{CH}_2\text{CH}_2-$), 3.18-3.41 (m, 2H, $-\text{CH}_2\text{N}(\text{CH}_3)\text{CH}_2\text{CH}_2-$), 4.74-4.87 ppm (m, 2H, $-\text{CH}_2\text{N}(\text{CH}_3)\text{CH}_2\text{CH}_2-$); ^{13}C -NMR (50 MHz, D_2O): δ = 16.4 (t, $^2J_{\text{PC}}$ = 7.3 Hz), 27.4, 38.2, 45.7, 54.9, 70.2 (t, $^1J_{\text{PC}}$ = 140 Hz), 144.9, 145.9, 157.3 ppm. Anal. calcd for $\text{C}_9\text{H}_{17}\text{NaN}_4\text{O}_9\text{P}_2 \cdot 1.14 \text{ H}_2\text{O}$: C 25.10%, H 4.51%, N 13.01%, found: C 25.50%, H 4.65%, N 12.60%.

4.1.6.4

[4-(*N*-Methyl-*N*-(3-carbamoylfuroxan-4-yl)methyl)-1-hydroxybutylidene]bis(phosphonic)acid

(25a). 40% yield. ^1H NMR (200 MHz, D_2O): δ = 1.81-2.04 (m, 4H, $-\text{CH}_2\text{CH}_2\text{C}(\text{OH})[\text{PO}(\text{OH})_2]_2$), 2.89 (s, 3H, $-\text{CH}_2\text{N}(\text{CH}_3)\text{CH}_2\text{CH}_2-$), 3.29 (br t, 2H, $-\text{CH}_2\text{N}(\text{CH}_3)\text{CH}_2\text{CH}_2-$), 4.70 ppm (covered by the solvent peak, 2H, $-\text{CH}_2\text{N}(\text{CH}_3)\text{CH}_2\text{CH}_2-$); ^{13}C NMR (50 MHz, D_2O): δ = 16.4 (t, $^2J_{\text{PC}}$ = 6.7 Hz), 27.4, 38.2, 47.7, 55.1, 70.2 (t, $^1J_{\text{PC}}$ = 140.0 Hz), 108.5, 147.4, 155.1 ppm. Anal. calcd for $\text{C}_9\text{H}_{18}\text{N}_4\text{O}_{10}\text{P}_2 \cdot 1.5 \text{ H}_2\text{O}$: C 25.07%, H 4.91%, N 12.99%, found: C 25.27%, H 4.82%, N 12.63%.

4.1.7 Determination of $\text{p}K_{\text{a}}$ values

Potentiometric titrations of compounds were performed with the GlpKa apparatus (Sirius Analytical Instruments Ltd., Forest Row, East Sussex, UK). Ionization constants were determined as outlined in literature: the aqueous titrations were carried out under N_2 at 25.0 ± 0.1 °C, and final data were obtained with the Multiset approach.³⁵ Ionization constant measurement of compounds **24**, **24a**, **25**, **25a** was repeated in different methanol-water mixtures (18-40% wt); aqueous $\text{p}K_{\text{a}}$ values were obtained by extrapolation at 0% methanol using the Yasuda-Shedlovsky procedure.²²

4.1.8 Adsorption of BPs to HAP

HAP (150 mg, Aldrich) was equilibrated in 50 mL of 0.05 M Tris-HCl pH 7.4 for 24 h at 37 °C according to literature.^{17,19} The BPs (1 mM) were incubated in HAP suspension at 37 °C and magnetically stirred. After 0 h, 6 h and 24 h, 1 mL of suspension was centrifuged (10000 rpm, 10 min), and the concentration of the BPs in the supernatant was determined by RP-HPLC. The HPLC system consisted of an Agilent

1200 chromatograph system equipped with a multiple wavelength detector SL (Agilent) and a ZORBAX Eclipse XDB C18 column (150 × 4 mm, 5 µm, Agilent). The mobile phase consisted of methanol/10 mM phosphate buffer pH 7.4 containing 1 mM tetrabutylammonium hydrogen sulfate (60/40 v/v for compounds **12**, **12a**, **13**, **13a**, **19**, **19a**, **20**, **20a**; 40/60 v/v for compounds **24**, **24a**, **25**, **25a**). The flow-rate was 1.2 mL/min, and the injection volume was 20 µL (Rheodyne, Cotati, CA). The peaks were monitored at 226 nm.

4.2 Biological methods

Recombinant human M-CSF was purchased from R&D Systems (Abingdon, UK) and recombinant human RANKL was from Alexis (San Diego, CA). Samples from peripheral blood (PB) were obtained from healthy controls, showing normal bone metabolism (evaluated by bone densitometry). In order to enrol a homogeneous group of healthy controls we adopted the following exclusion criteria: chronic diseases; therapies with medications which could increase osteoclastogenesis (steroids, glucocorticoids); therapies with calcium, vitamin D, phosphorus. Informed consent was obtained to comply with institutional policies.

4.2.1 Cell cultures

PBMCs, collected from healthy controls, were isolated after centrifugation over a density gradient (Lymphoprep, Nycomed Pharma, Norway) and cultured in a 24-well plate at a density of $2 \cdot 10^6$ cells mL⁻¹ in α -MEM (Invitrogen, UK) supplemented with 10% Fetal Bovin Serum (FBS, BioWhittaker, Walkersville, MD), penicillin (100 U mL⁻¹) and streptomycin (100 µg mL⁻¹). To obtain fully differentiated human OCs, PBMCs were then cultured with/without M-CSF (25 ng mL⁻¹) from day 0 and RANKL (30 ng mL⁻¹) from day 10. Culture supernatants were changed on days 5 and 10, when medium was either refreshed and supplemented or not with the agents described above. They were all prepared as stock solutions at 10^{-3} M concentration in distilled water, aliquoted and stored at -20 °C. Cultures were stopped

after 15 days, mature OCs were identified as multinucleated cells containing three or more nuclei and positive for the expression of TRAP and $\alpha V\beta 3$ (vitronectin receptor).

4.2.2 Culture of RAW 246.7 cells

As a model system of osteoclastogenesis we have used a clone of RAW 246.7 murine monocyte/macrophagic cell line (TIB-71), purchased from American Type Culture Collection (ATCC, Rockville, MD). RAW 246.7 cells were cultured in a 24-well plate at a density of $1 \cdot 10^4$ cell mL^{-1} in α -MEM (Invitrogen, UK) supplemented with 10% Fetal Bovin Serum (FBS, BioWhittaker, Walkersville, MD), penicillin (100 U mL^{-1}) and streptomycin ($100 \mu\text{g mL}^{-1}$). After 24 h of culture, media were changed and replaced by one containing RANKL (30 ng mL^{-1}) and tested compounds. At day 3 media were removed and cells were washed with PBS and subsequently fixed for 30 min in a solution of 4% paraformaldehyde and stained for tartrate-resistant acid phosphatase solution (TRAP, Sigma) according to the manufacturer.

4.2.3 Microsomal enzyme preparation

Cellular fractions ($10,000 \times \text{g}$, $100,000 \times \text{g}$ supernatants and microsomes, respectively) of rat liver were prepared as described by Popjak.³⁶ All procedures were performed at 4°C . Briefly, livers were homogenized in 2.5 volumes of 0.1 M potassium phosphate buffer, pH 7.4, containing 5 mM MgCl_2 and 30 mM nicotinamide. Homogenates were centrifuged at $10,000 \times \text{g}$ for 30 min and the $10,000 \times \text{g}$ supernatant (S10) was aliquoted and stored at -80°C . To obtain the microsomes, the S10 was further centrifuged at $100,000 \times \text{g}$ for 60 min. The pelleted microsomes were resuspended in one-tenth volume of the original homogenate. Microsomes and $100,000 \times \text{g}$ supernatant (S100) were aliquoted and stored at -80°C . Proteins were assayed by the BCA method (Pierce) using bovine serum albumin as a standard.

4.2.4 Inhibition of the section of sterol biosynthesis ranging from mevalonic acid to squalene in rat liver S10 or S100 cellular fractions

For the inhibition test, bisphosphonates **12**, **12a**, **20**, **20a** were dissolved in methanol and sodium ibandronate, tested as a reference inhibitor, was dissolved in 0.1 M sodium phosphate buffer, pH 7.4 (PBS). Rat liver S10 or S100 were incubated with (*R,S*)-[2-¹⁴C]mevalonic acid (0.05 μ Ci, 55 mCi mmol⁻¹, 2.04 GBq mmol⁻¹) (Amersham Pharmacia Biotech, UK), in the presence of 0.2 mM U14266A, an oxidosqualene cyclase inhibitor.³⁷ The labelled substrate, U14266A, bisphosphonates **12**, **12a**, **20**, **20a** were added as organic solution to test tubes containing Tween-80 (final concentration 0.2 mg mL⁻¹) and the solvent was evaporated under a stream of nitrogen. Residues were redissolved in 50 μ L of PBS, containing 5 mM MgCl₂, 4 mM MnCl₂, 30 mM nicotinamide, 2 mM ATP. 50 μ L of S10 or S100 (2 mg protein) were then added to test tubes. Assay tubes were flushed with N₂, capped, and incubated at 30 °C for 60 min. The inhibition by sodium ibandronate was tested under the same conditions, except for the addition of the inhibitor, which was directly transferred as a PBS solution into the test tubes containing the reaction mixture freed from solvent. The enzymatic reaction was stopped by adding 20 μ L of 5 M HCl and the mixture was kept at 37 °C for 30 min to complete the hydrolysis of prenol pyrophosphate. Hydrolysis products were extracted twice with petroleum ether (1.5 and 1 mL). Extracts were spotted on TLC plates (Alufolien Kieselgel 60F254, Merck, Darmstadt, Germany) using benzene/acetone (90/10 v/v) as the developing solvent, and authentic standards of geraniol, farnesol, squalene, oxidosqualene, lanosterol and cholesterol as reference compounds. Labelled metabolites were determined by scanning TLC plates with a System 200 Imaging Scanner (Hewlett-Packard, Palo Alto, CA, USA). Prenol references were detected by iodine vapour. Under our experimental conditions (plugged test tubes with no NADPH added, in the presence of an oxidosqualene cyclase inhibitor) only one major radioactive product (about 80% of total extract radioactivity) co-chromatographing with squalene was detected in control tests (no bisphosphonate inhibitors) incubated with the S10 cellular fraction.

4.2.5 Inhibition of squalene synthase activity in rat liver microsomes

The substrate [1-³H]-FPP (0.02 μ Ci, 26.2 Ci mmol⁻¹, 969.4 GBq mmol⁻¹) (PerkinElmer Life and Analytical Science), 0.2 mM U14266A (oxidosqualene cyclase inhibitor) and different concentrations of

bisphosphonates, dissolved in methanol, were added to test tubes containing Tween-80 (final concentration 0.2 mg mL⁻¹). To the mixture freed from solvent and redissolved in 50 µL of PBS containing 5 mM MgCl₂, 30 mM nicotinamide, 20 mM NaF and 2 mM NADPH, 50 µL of microsomes (3 mg protein) were added. Sodium ibandronate, dissolved in PBS, was used as reference inhibitor. Assay tubes were flushed with N₂, capped, and incubated at 30 °C for 60 min. The enzymatic reaction was stopped by adding methanolic KOH (1 mL, 10% w/v) and heating at 80 °C for 30 min in a water bath. The reaction mixture was extracted twice with petroleum ether (1.5 and 1 mL) and the synthesized [³H]-squalene was counted in Ready Gel™ (Beckman) using a Packard liquid scintillation counter. Control incubations were carried out in the same conditions, in the absence of bisphosphonate inhibitors. The efficiency of the petroleum ether extraction was about 90%, as indicated by the recovery of [¹⁴C]-squalene added at the end of the enzymatic reaction as a tracer. Extracts from both control and inhibition tests were analysed by TLC, using cyclohexane/ethyl acetate (85/15, v/v) as a developing solvent and authentic standards of cholesterol, lanosterol, oxidosqualene, and squalene as reference compounds. Labelled products were determined by scanning with a System 200 Imaging Scanner (Hewlett-Packard, Palo Alto, CA, USA). The radiochromatographic analysis showed that, in the control test, 95% of radioactivity accumulated into a single peak co-chromatographing with squalene. In order to calculate the IC₅₀ values, the results were expressed as % of radioactivity extracted with respect to the control incubations in the absence of inhibitors.

4.2.6 Statistical analyses

Statistical analyses were performed with Prism 5.0. We compared the results by means of Student's paired t-test. The results were considered statistically significant for $p < 0.05$. IC₅₀ values (inhibitor concentrations that decreased enzymatic conversion by 50%) relative to squalene synthase activity were calculated by nonlinear regression analysis of the residual activity versus the log of inhibitor concentration using statistical software XLfit 5.1 from IDBS (Guildford, Surrey, UK).

4.2.7 Vasodilator activities

Thoracic aortas were isolated from male Wistar rats weighing 180-200 g. As few animals as possible were used. The purposes and the protocols of our studies were approved by the Ministero della Salute, Rome, Italy. The endothelium was removed and the vessels were helically cut: three strips were obtained from each aorta. The tissues were mounted under 1.0 g tension in organ baths containing 30 mL of Krebs-bicarbonate buffer with the following composition (mM): NaCl 111.2, KCl 5.0, CaCl₂ 2.5, MgSO₄ 1.2, KH₂PO₄ 1.0, NaHCO₃ 12.0, glucose 11.1, maintained at 37 °C and gassed with 95% O₂-5% CO₂ (pH = 7.4). The aortic strips were allowed to equilibrate for 120 min and then contracted with 1 μM L-phenylephrine. When the response to the agonist reached a plateau, cumulative concentrations of the vasodilating agent were added. Results are expressed as EC₅₀ ± SE (μM). The effects of 1 μM ODQ on relaxation were evaluated in separate series of experiments. ODQ was added to the organ bath 5 minutes before the contraction. Responses were recorded by an isometric transducer connected to the MacLab System PowerLab (ADInstruments Ltd, Oxfordshire, UK). Addition of the drug vehicle (DMSO) had no appreciable effect on contraction level.

4.3 Molecular modelling

The molecular models of ibandronate, **20** and **20a** were constructed using standard bond lengths and angles with the MOE software package.³⁸ In accordance with their pK_a values (Table 1), all compounds were modelled with three of the four phosphonate hydroxyl groups in their ionized state; in the case of ibandronate the basic nitrogen atom was modelled as protonated. Following truncated Newton-Raphson geometry optimization with the MMFF94s force field (MMFF94 charges, GB/SA implicit solvent model) until the gradient was lower than 0.001 kcal mol⁻¹ Å⁻¹, a Monte Carlo conformational search was carried out with the StochasticCSearch module implemented in MOE. The most stable conformer was then chosen for further optimization by an ab initio HF/6-31G(d) method using the GAMESS-US package,³⁹ on the equilibrium geometry, atom-centred point charges were derived by fitting the quantum-mechanical

electrostatic potential with the RESP method.⁴⁰ The experimental X-ray structures of human FPPS in complex with ibandronate (PDB ID 2F94), human SQS in complex with CP-320473 (PDB ID 1EZF) and human GGPPS in complex with geranylgeranyl diphosphate (PDB ID 2Q80) were retrieved from the Protein Data Bank.⁴¹ While only one monomer is present in the FPPS asymmetric unit, a trimer and an hexamer are found for SQS and GGPPS, respectively. Since neither active site involves the interface between monomers, only one monomer was considered. Two short loops are missing from the crystal structure of SQS and GGPPS (10-aminoacid and 6-aminoacid long, respectively). Since these loops do not contribute to defining the shape of the active sites they were not modelled; rather, the *C*- and *N*- chain terminals at the boundaries of the missing segments were simply capped with a *N*-methanamide and an acetyl group, respectively. After removing co-crystallized inhibitors, missing hydrogen atoms were added to the three enzymes in standard positions, then their coordinates were optimized with the SANDER module of the AMBER 10 software package,⁴² while heavy atoms were harmonically restrained to the initial X-ray crystal positions with a force constant of 1000 kcal mol⁻¹ Å⁻². All molecular mechanics optimizations on the proteins were accomplished using parameters and electrostatic charges of the AMBER99 force field. The volume of the active sites was computed with the VOIDOO program.⁴³ Docking of the inhibitors was carried out using AutoDock 4.0.1.⁴⁴⁻⁴⁶ A grid with a 0.375 Å step size was centred on the active site and energy maps were pre-calculated with AutoGrid, then flexible docking was carried out with AutoDock. The target proteins were kept rigid, while ligands were left free to explore the conformational space inside the enzyme cavities; 200 separate docking simulations were run on each target using the Lamarckian genetic algorithm with default parameters. Docking poses were clustered according to their RMS deviation from the starting reference structure.

5. Acknowledgements

This work was supported by a grant from Regione Piemonte (Ricerca sanitaria finalizzata 2008).

6. References

1. Fleisch, H. *Bisphosphonates in Bone Diseases*, 3rd ed.; The Parthenon Publishing Group Inc.: New York, 1997.
2. Boyle, W. J.; Simonet, W. S.; Lacey, D. L. *Nature* **2003**, *423*, 337.
3. Russell, R. G. G.; Croucher, P. I.; Rogers, M. J. *Osteoporosis Int.* **1999**, *9*, 66.
4. Dunford, J. E.; Kwaasi, A. A.; Rogers, M. J.; Barnett, B. L.; Ebetino, F. H.; Russell, R. G. G.; Oppermann, U.; Kavanagh, K. L. *J. Med. Chem.* **2008**, *51*, 2187.
5. Green, J. R.; Clezardin, P. *Am. J. Clin. Oncol. (CCT)* **2002**, *25*, S3.
6. Rogers, M. J.; Frith, J. C.; Luckman, S. P.; Coxon, F. P.; Benford, H. L.; Mönkkönen, J.; Auriola, S.; Chilton, K. M.; Russell, R. G. G. *Bone* **1999**, *24*, 73S.
7. Wildler, L.; Jaeggi, K. A.; Glatt, M.; Müller, K.; Bachmann, R.; Bisping, M.; Born, A.-R.; Cortesi, R.; Guiglia, G.; Jeker, H.; Klein, R.; Ramseier, U.; Schmid, J.; Schreiber, G.; Seltenmeyer, Y.; Green, J. R. *J. Med. Chem.* **2002**, *45*, 3721.
8. Szabo, C. M.; Matsumura, Y.; Fukura, S.; Martin, M. B.; Sanders, J. M.; Sengupta, S.; Cieslak, J. A.; Loftus, T. C.; Lea, C. R.; Lee, H.-J. Koohang, A.; Coates, R. M.; Sagami, H.; Oldfield, E. *J. Med. Chem.* **2002**, *45*, 2185.
9. Reszka, A.; Rodan, G. A. *Curr. Rheumatol. Rep.* **2003**, *5*, 65.
10. Ylitalo, R. *Gen. Pharmacol.* **2002**, *35*, 287.
11. McFarlane, S. I.; Muniyappa, R.; Shin, J. J.; Bahtiyar, G.; Sowers, J. R. *Endocrine* **2004**, *23*, 1.
12. Hamerman, D. *Q. J. Med.* **2005**, *98*, 467.
13. Gasco, A.; Schoenafinger K. In *Nitric Oxide Donors*; Wang, P.G.; Cai, T. B.; Taniguchi, N., Eds.; Wiley-VCH Verlag GmbH & Co KGaA: Weinheim, 2005; pp 131-175.
14. Kerwin Jr, J. F.; Lancaster, J. R.; Feldman, P. L. *J. Med. Chem.* **1995**, *38*, 4343.
15. *Nitric Oxide and the Cardiovascular System*; Loscalzo, J.; Vita J. A., Eds.; Humana Press: Totowa, New Jersey, 2000.
16. Wallace, J. L. *Br. J. Pharmacol.* **2007**, *152*, 421.
17. Van't Hof, R. J.; Ralstone, S. H. *Immunology* **2001**, *103*, 255.

18. Cummings, S. R.; Schwartz, A. V.; Black, D. M. *N. Engl. Med.* **2007**, 356, 1895.
19. Defilippi, A.; Sorba, G.; Calvino, R.; Garrone, A.; Gasco, A.; Orsetti, M. *Arch. Pharm. (Weinheim)* **1988**, 321, 77.
20. Nancollas, G. H.; Tang, R.; Phipps, R. J.; Henneman, Z.; Gulde, S.; Wu, W.; Mangood, A.; Russell, R. G. G.; Ebetino, F. H. *Bone* **2006**, 38, 617.
21. Lazzarato, L.; Rolando, B.; Lolli, M. L.; Tron, G. C.; Fruttero, R.; Gasco, A.; Deleide, G.; Guenther, H. L. *J. Med. Chem.* **2005**, 48, 1322.
22. Avdeef, A.; Comer, J. E. A.; Thompson, S. J. *Anal. Chem.* **1993**, 65, 42.
23. Cohen, H.; Solomon, V.; Alferiev, I. S.; Breuer, E.; Ornoy, A.; Patlas, N.; Eidelman, N.; Hägele, G.; Golomb, G. *Pharm. Res.* **1998**, 15, 606.
24. Rondeau, J.-M.; Bitsch, F.; Bourgier, E.; Geiser, M.; Hemmig, R.; Kroemer, M.; Lehmann, S.; Ramage, P.; Rieffel, S.; Strauss, A.; Green, J. R.; Jahnke, W. *ChemMedChem* **2006**, 1, 267.
25. Pandit, J.; Danley, D. E.; Schulte, G. K.; Mazzalupo, S.; Pauly, T. A.; Hayward, C. M.; Hamanaka, E. S.; Thompson, J. F.; Harwood Jr., H. J. *J. Biol. Chem.* **2000**, 275, 30610.
26. Kavanagh, K. L.; Dunford, J. E.; Bunkoczi, G.; Russell, R. G.; Oppermann, U. *J. Biol. Chem.* **2006**, 281, 22004.
27. Di Stilo, A.; Chegaev, K.; Lazzarato, L.; Fruttero, R.; Gasco, A.; Rastaldo, R.; Cappello, S. *Arzneim. Forsch.* **2009**, 59, 111.
28. Jork, H.; Funk, W.; Fischer, W.; Wimmer, H. *Thin layer chromatography*, VCH, Weinheim, Germany, **1990**, vol. 1a, pp. 170.
29. Calvino, R.; Mortarini, V.; Gasco, A.; Sanfilippo, A.; Ricciardi, M. L. *Eur. J. Med. Chem.* **1980**, 15, 485.
30. Boschi, D.; Di Stilo, A.; Cena, C.; Lolli, M. L.; Fruttero, R.; Gasco, A. *Pharm. Res.* **1997**, 14, 1750.
31. Sorba, G.; Ermondi, G.; Fruttero, R.; Galli, U.; Gasco, A. *J. Heterocyclic Chem.* **1996**, 33, 327.

32. Bertinaria, M.; Galli, U.; Sorba, G.; Fruttero, R.; Gasco, A.; Brenciaglia, M. I.; Scaltrito, M. M.; Dubini, F. *Drug. Dev. Res.* **2003**, *60*, 225.
33. Kieczkowski, G. R.; Jobson, R. B.; Melillo, D. G.; Reinhold, D. F.; Grenda, V. J.; Shinkai, I. *J. Org. Chem.* **1995**, *60*, 8310.
34. Di Stilo, A.; Visentin, S.; Cena, C.; Gasco, A. M.; Ermondi, G.; Gasco, A. *J. Med. Chem.* **1998**, *41*, 5393.
35. Avdeef, A. *J. Pharm. Sci.* **1993**, *82*, 183.
36. Popjak, G. *Methods Enzymol.* **1969**, *15*, 393.
37. Field, R. B.; Holmlund, C. E.; Whittaker, N. F. *Lipids* **1979**, *14*, 741.
38. MOE version 2008.10, Chemical Computing Group Inc., Montreal, Quebec, Canada, 2008.
39. Schmidt, M. W.; Baldrige, K. K.; Boatz, J. A.; Elbert, S. T.; Gordon, M. S.; Jensen, J. H.; Koseki, S.; Matsunaga, N.; Nguyen, K. A.; Su, S. J.; Windus, T. L.; Dupuis, M.; Montgomery, J. A. *J. Comput. Chem.* **1993**, *14*, 1347.
40. Wang, J.; Cieplak, P.; Kollman, P. A. *J. Comput. Chem.* **2000**, *21*, 1049.
41. The RCSB Protein Data Bank, <http://www.rcsb.org/> (Last accessed January 29, 2010).
42. AMBER 10, Case, D. A.; Darden, T. A.; Cheatham III, T. E.; Simmerling, C. L.; Wang, J.; Duke, R. E.; Luo, R.; Crowley, M.; Walker, R. C.; Zhang, W.; Merz, K. M.; Wang, B.; Hayik, S.; Roitberg, A.; Seabra, G.; Kolossvary, I.; Wong, K. F.; Paesani, F.; Vanicek, J.; Wu, X.; Brozell, S. R.; Steinbrecher, T.; Gohlke, H.; Yang, L.; Tan, C.; Mongan, J.; Hornak, V.; Cui, G.; Mathews, D. H.; Seetin, M. G.; Sagui, C.; Babin, V.; Kollman, P. A. University of California, San Francisco (USA), 2008.
43. Kleywegt, G. J.; Jones, T. A. *Acta Cryst.* **1994**, *D50*, 178.
44. Goodsell, D. S.; Olson, A. J. *Proteins* **1990**, *8*, 195.
45. Morris, G. M.; Goodsell, D. S.; Huey, R.; Olson, A. J. *J. Comput. Aid. Mol. Des.* **1996**, *10*, 293.
46. Morris, G. M.; Goodsell, D. S.; Halliday, R. S.; Huey, R.; Hart, W. E.; Belew, R. K.; Olson, A. J. *J. Comput. Chem.* **1998**, *19*, 1639.

Table 1. pK_a values and affinity for HAP of ibandronate and of final bisphosphonates

Compd	Dissociation constants					Affinity to HAP ^a		
	pK_{a1}	$pK_{a2} \pm SD$	$pK_{a3} \pm SD$	$pK_{a4} \pm SD$	$pK_{a5} \pm SD$	0 h	6 h	24 h
5^b	-	2.84	6.08	9.80	10.43	71 \pm 2	56 \pm 1	56 \pm 3
12	< 1.5	2.81 \pm 0.02	6.88 \pm 0.01	11.4 \pm 0.1	-	75 \pm 3	54 \pm 3	44 \pm 1
12a	< 1.5	2.67 \pm 0.02	6.86 \pm 0.01	11.2 \pm 0.1	-	76 \pm 1	51 \pm 2	44 \pm 2
13	< 1.5	2.69 \pm 0.04	7.00 \pm 0.03	10.7 \pm 0.1	-	64 \pm 2	48 \pm 4	40 \pm 5
13a	< 1.5	2.64 \pm 0.03	6.87 \pm 0.02	11.6 \pm 0.1	-	70 \pm 2	57 \pm 2	42 \pm 3
19	< 1.5	2.69 \pm 0.04	6.66 \pm 0.02	11.0 \pm 0.2	-	56 \pm 1	40 \pm 4	33 \pm 2
19a	< 1.5	2.90 \pm 0.02	6.86 \pm 0.01	11.2 \pm 0.1	-	59 \pm 4	36 \pm 3	27 \pm 2
20	< 1.5	2.80 \pm 0.05	6.64 \pm 0.03	10.6 \pm 0.1	-	56 \pm 2	41 \pm 1	34 \pm 1
20a	< 1.5	2.52 \pm 0.03	6.65 \pm 0.01	11.3 \pm 0.1	-	59 \pm 2	42 \pm 1	33 \pm 2
24	< 1.5	2.05 \pm 0.06	6.05 \pm 0.01	7.45 \pm 0.02	11.1 \pm 0.1	69 \pm 2	54 \pm 1	46 \pm 1
24a	< 1.5	2.26 \pm 0.07	5.89 \pm 0.01	7.13 \pm 0.01	11.2 \pm 0.1	69 \pm 2	51 \pm 4	46 \pm 2
25	< 1.5	2.04 \pm 0.09	6.02 \pm 0.02	7.65 \pm 0.03	11.0 \pm 0.1	70 \pm 2	51 \pm 2	52 \pm 2
25a	< 1.5	2.16 \pm 0.06	6.03 \pm 0.01	7.36 \pm 0.01	10.8 \pm 0.1	62 \pm 1	49 \pm 2	46 \pm 1

^a Percentage of residual BP in solution; all values are expressed as mean \pm SD, n = 4-6.^b Dissociation constants reported in literature.¹⁹

Table 2. Inhibitory effect of compounds **5**, **12**, **12a**, **20**, **20a** on squalene synthase enzyme in rat liver microsomes

Compd	IC ₅₀ [μM] ^a
5	0.64 ± 0.16
12	17.68 ± 1.72
12a	22.95 ± 3.57
20	3.71 ± 0.42
20a	7.95 ± 2.23

^a Data expressed as mean ± SE (three different experiments in duplicate).

Table 3. Vasodilating activity of compounds **5**, **12a**, **13a**, **19a**, **20a**, **24a**, **25a**

Compounds	EC ₅₀ [μM] ^a	EC _{50ODQ} [μM] ^b
5	inactive	not tested
12a	73 ± 18	^c
13a	0.20 ± 0.03	193 ± 36
19a	108 ± 20	^c
20a	0.23 ± 0.03	192 ± 27
24a	45 ± 3	^c
25a	35 ± 2	^c

^a Data expressed as mean ± SE, n = 3-15.

^b Experiments performed in the presence of 1 μM ODQ.

^c At the maximal concentration tested (1·10⁻⁴ M) vasodilation does not reach 50%.

Figure legends

Figure 1. Structures of bisphosphonic acids (**1**), pyrophosphoric acid (**2**) and examples of first (etidronate, **3**), second (alendronate, **4**; ibandronate, **5**) and third generation (zoledronate, **6**) bisphosphonates.

Figure 2. TRAP⁺ RAW-OCs number. The number of TRAP⁺ RAW-OCs containing three or more nuclei/cell were quantified from three independent experiments. Data are presented as the mean \pm SD; statistical differences from controls not treated with N-BPs (10 μ M): * $p < 0.001$; ** $p < 0.00001$. The result of an ANOVA statistical test is 0.0001.

Figure 3 TRAP⁺ MNC number. The number of TRAP⁺ OCs containing three or more nuclei/cell were quantified from nine independent wells per condition. Data are presented as the mean \pm SD; statistical differences from controls not treated with N-BPs (10 μ M): * $p < 0.05$; ** $p < 0.002$. The result of an ANOVA statistical test is 0.0001.

Figure 4. Ibandronate (thicker lines) and compound **20** (thinner lines) docked in FPPS (a), SQS (b) and GGPPS (c), respectively. Polar hydrogens have been omitted for clarity. The solvent-excluded surface of the cavity has been included to evidence how bisphosphonates **20** and **20a** partially protrude from the FPPS cavity, while they are well accommodated in the active sites of SQS and GGPPS.

Figure 5. Concentration-response curves of **20a** in the absence and in the presence of 1 μ M ODQ.

Scheme 1. a) *t*-BuO⁻K⁺, dry THF, -15 °C for compounds **10**, **10a**, -45 °C for compounds **11**, **11a**; b) TMSBr, CH₂Cl₂; c) MeOH, 0 °C to rt.

Scheme 2. a) 1,5-Pentanediol, NaOH 50% w/w, THF; b) Jones reagent, acetone, 0 °C to rt; c) SOCl₂; d) P(OMe)₃, dry THF, 0 °C to rt; e) HPO(OMe)₂, Et₂NH, dry THF, 0 °C to rt; f) TMSBr, CH₂Cl₂; g) MeOH, 0 °C to rt.

Scheme 3. a) 2 M NaOH, pH 12, H₂O, CH₃CN.

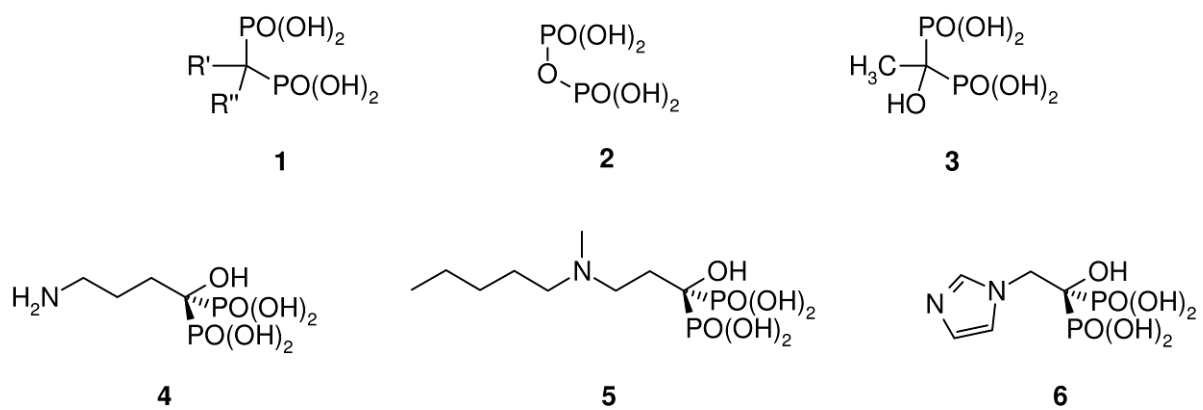


Figure 1.

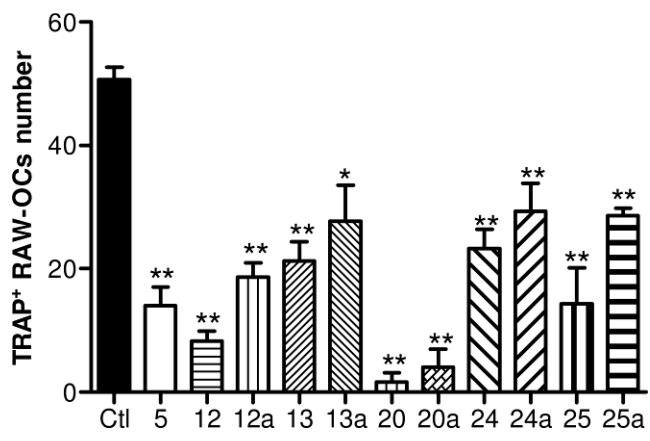


Figure 2.

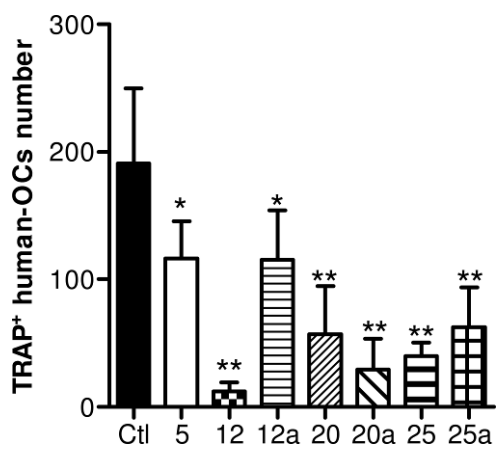


Figure 3.

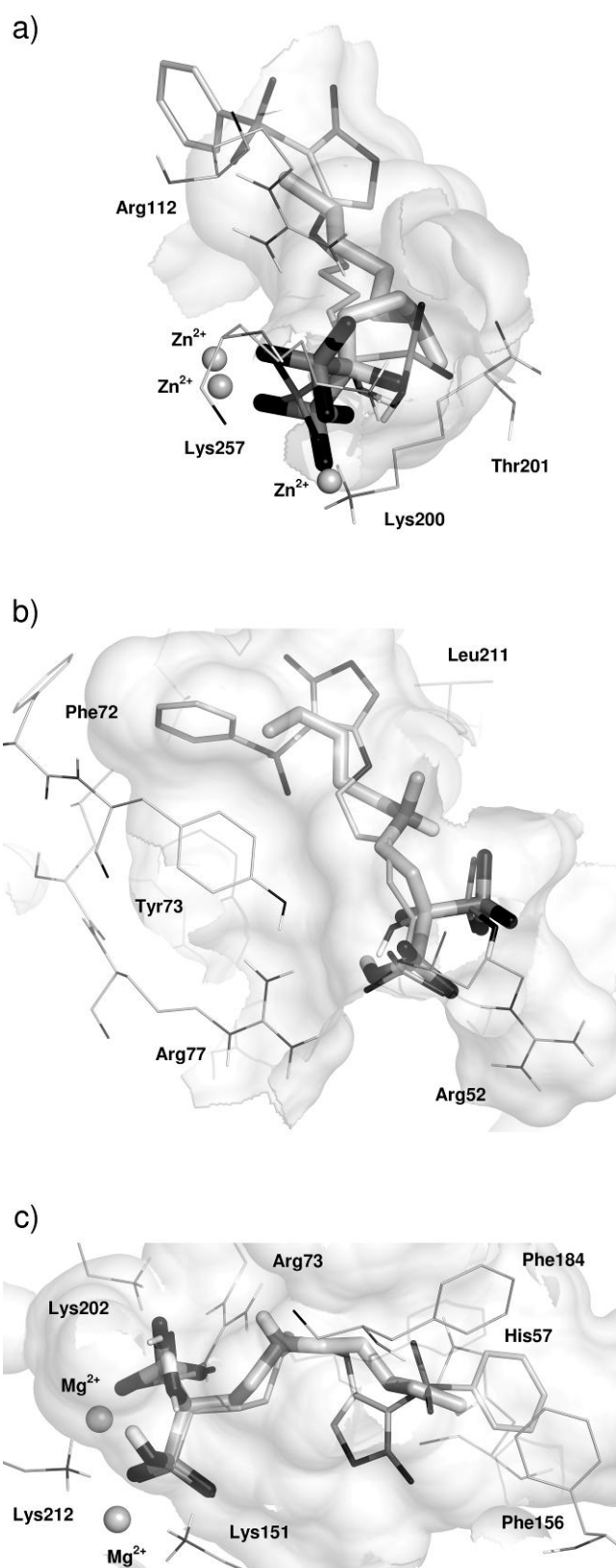


Figure 4.

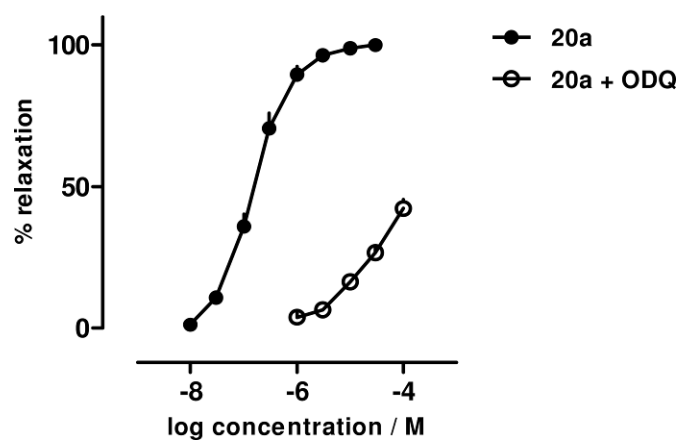
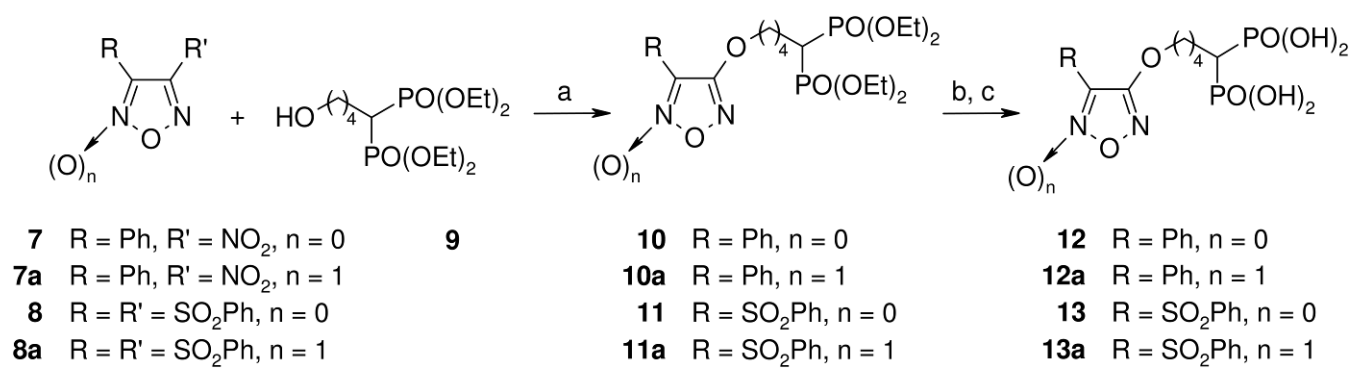
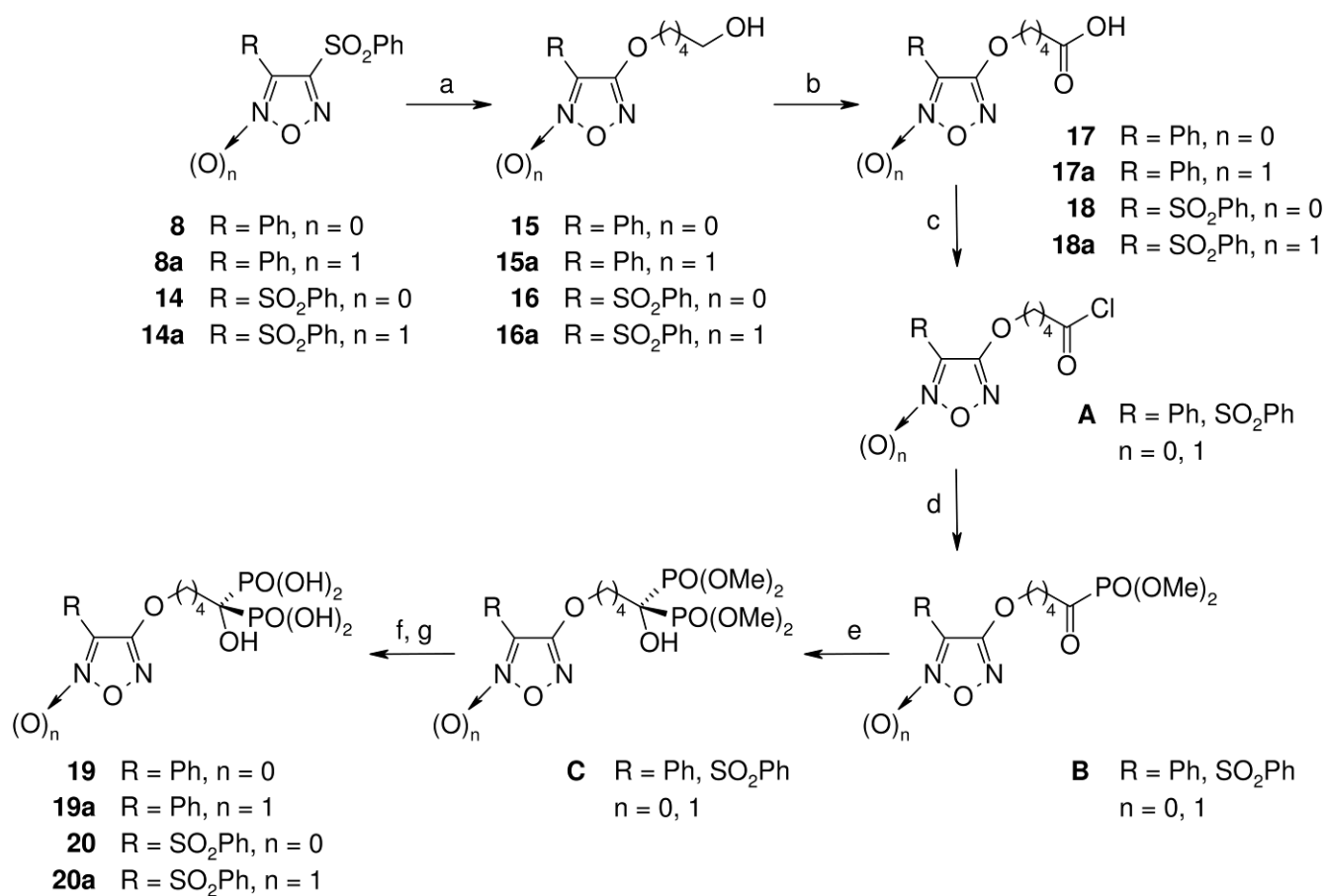


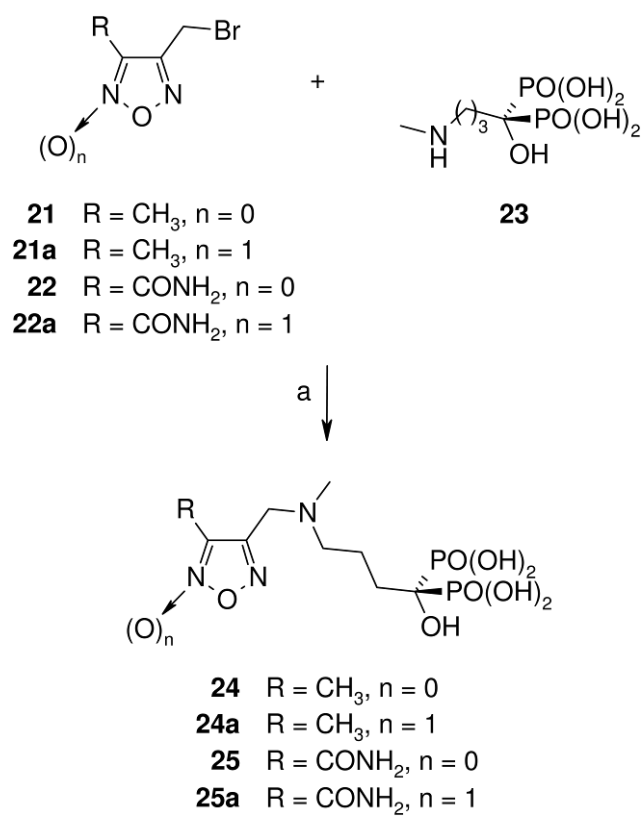
Figure 5.



Scheme 1.



Scheme 2.



Scheme 3.